Available online at www.sciencedirect.com
ScienceDirect
Physics Procedia 3 (2010) 5–16
Physics Procedia
www.elsevier.com/locate/procedia

International Congress on Ultrasonics, Universidad de Santiago de Chile, January 2009

Introduction to Nonlinear Acoustics

Leif Bjørnø*

UltraTech Holding, Stendiget 19, DK-2630 Taastrup, Denmark.

Abstract

A brief review of the basic principles of fluid mechanics needed for development of linear and nonlinear ultrasonic concepts will be given. The fundamental equations of nonlinear ultrasonics will be derived and their physical properties explained. It will be shown how an originally monochromatic finite-amplitude ultrasonic wave, due to nonlinear effects, will distort during its propagation in time and space to form higher harmonics to its fundamental frequency. The concepts of shock formation will be presented. The material nonlinearity, described by the nonlinearity parameter B/A of the material, and the convective nonlinearity, described by the ultrasonic Mach Number, will be explained. Two procedures for determination of B/A will briefly be described and some B/A-values characterizing biological materials will be presented. Shock formation, described by use of the Goldberg Number,and Ultrasonic Saturation will be discussed.. An introduction to focused ultrasonic fields will be given and it will be shown how the ultrasonic intensity will vary axially and laterally in and near the focal region and how the field parameters of interest to biomedical applications may be described by use of the KZK-Model. Finally, an introduction will be given to the parametric acoustic array formed by mixing and interaction of two monochromatic, finite-amplitude ultrasonic waves in a liquid and the potentials of this mixing process in biomedical ultrasound will briefly be mentioned.

Keywords: Fundamental equations; nonlinear distortion; second-order nonlinearity parameter B/A; biological materials; ultrasonic Mach Number; Gol'dberg Number, ultrasonic saturation; focused ultrasonic fields; the K-Z-K model, parametric acoustic arrays.

1. Introduction

The real World, we live in, is nonlinear. Relations for instance between characteristic parameters like pressure, density, temperature etc. in fluids and relations between material constants in solids are nonlinear. Since Robert Hooke (1635 – 1703) put forward his linear elastic relation (named: Hooke's Law) between force and deformation of solids, attempts have been made to "linearize" the World. The driving force behind the linearization has in particular been lack of fundamental understanding of the nonlinearity concepts and lack of tools to handle nonlinear problems. Only the strong development in computer technology, faster and more powerful computers developed

* Corresponding author. Tel.: +45-43-99 52 84; fax: +45-43-52 26 71.
E-mail address: prof.lb@mail.dk.

doi:10.1016/j.phpro.2010.01.003

over the last 40 – 50 years, have given access to understanding and exploitation of nonlinear phenomena. One of these phenomena is ***Nonlinear Ultrasonics.***

2. Fundamental equations

The fundamental equations of nonlinear ultrasonics may be derived from the fundamental equations of Fluid Mechanics, namely the ***Equation of Continuity***, the ***Equations of Motions*** and the ***Equation of Energy***. To these 5 equations – the Equations of Motions consist of an equation in each of the 3 coordinate directions - comes a 6th equation, a constitutive equation named the ***Equation of State***. All together we have 6 equations, which describe all types of motions in fluids. The Equations of Continuity, of Motions and of Energy are shown on Equations 1:

$$\frac{\partial \rho}{\partial t} + \frac{\partial}{\partial x_i}(\rho u_i) = 0$$

$$\rho\left(\frac{\partial u_i}{\partial t} + u_j \frac{\partial u_i}{\partial x_j}\right) = \rho F_i - \frac{\partial p}{\partial x_i} + \frac{\partial}{\partial x_j}\left[\eta\left(\frac{\partial u_i}{\partial x_j} + \frac{\partial u_j}{\partial x_i}\right)\right] + \frac{\partial}{\partial x_i}\left(\eta' \frac{\partial u_k}{\partial x_k}\right)$$

$$\rho c_v \frac{DT}{Dt} + \rho \frac{c_v(\gamma - 1)}{\beta} \frac{\partial u_i}{\partial x_i} + \frac{\partial q_i}{\partial x_i} - \Phi - q' = 0$$

Equations 1. Equation of Continuity, Equations of Motions and Equation of Energy, respectively.

Here p and ρ are the pressure {N/m^2} and the density {kg/m^3}, respectively. x_i and t denote the spatial coordinates (*i, j and k* = 1, 2 and 3) {m}, and time {s}, respectively. u_i is the particle velocity in the *i'th* direction {m/s}, F_i is an external body force {N/kg} in the *i'th* direction, and η and η' are the shear viscosity and the bulk viscosity {Ns/m^2}, respectively. T denotes the absolute temperature {^{o}K}, c_v is the specific heat for constant volume, and q_i is the rate of heat flux vector comprising conduction and radiation {N/sm}. q' is the internal heat production rate per unit volume {N/sm^2}, Φ is the viscous dissipation function {N/sm^2} and γ and β denote the ratio of specific heats and the isobaric compressibility.

If a so-called perturbation procedure is used, see Bjørnø [1], where the variables in the Equations of Continuity, of Motions and of Energy are replaced by the sum of their equilibrium values, with subscript *o*, and their first and second order variation components, subscripts *1* and *2*, respectively, as shown in Equations 2,

$$\rho = \rho_{(0)} + \rho_{(1)} + \rho_{(2)} + \ldots \quad \text{and} \quad T = T_{(0)} + T_{(1)} + T_{(2)} + \ldots$$

$$p(\rho, T) = p_{(0)}(\rho_{(0)}, T_{(0)}) + \left[\left(\frac{\partial p}{\partial \rho}\right)_T\right]_{(0)} (\rho - \rho_{(0)}) + \left[\left(\frac{\partial p}{\partial T}\right)_\rho\right]_{(0)} (T - T_{(0)}) + \ldots$$

$$u_i = 0 + u_{i(1)} + u_{i(2)} + \ldots$$

Equations 2. The perturbation procedure applied to the terms in Eqs. 1

where each term is the ***Acoustic Mach Number*** $M_a = u/c$ smaller than the previous one, the following 1st and 2nd order ultrasonic equations may be found as shown in Equations 3 for the 1st order ultrasonic equations and in Equations 4 for the 2nd order ultrasonic equations. c is the velocity of sound.

$$\frac{\partial \rho_{(1)}}{\partial t} + \rho_{(0)} \frac{\partial u_{i(1)}}{\partial x_i} = 0$$

$$\rho_{(0)} \frac{\partial u_{i(1)}}{\partial t} = -\frac{\partial p_{(1)}}{\partial x_i} + (\eta'_{(0)} + \eta_{(0)}) \frac{\partial}{\partial x_i}\left(\frac{\partial u_{k(1)}}{\partial x_k}\right) + \eta_{(0)} \frac{\partial^2 u_{i(1)}}{\partial x_j \partial x_j}$$

$$\frac{\partial T_{(1)}}{\partial t} = -\frac{(\gamma-1)}{\beta_{(0)}} \frac{\partial u_{i(1)}}{\partial x_i} + \frac{\kappa_{(0)}}{\rho c_v} \frac{\partial}{\partial x_i}\left(\frac{\partial T_{(1)}}{\partial x_i}\right) - q'' T_{(1)}$$

$$p_{(1)} = \frac{c_0^2}{\gamma}(\rho_{(1)} + \beta_{(0)} \rho_{(0)} T_{(1)})$$

$$c^2_{(0)} \equiv \left[\left(\frac{\partial p}{\partial \rho}\right)_s\right]_{(0)} \text{ and } \beta_{(0)} = -\frac{1}{\rho_{(0)}}\left[\left(\frac{\partial \rho}{\partial T}\right)_p\right]_{(0)}$$

Equations 3. The first-order ultrasonic equations.

$$\frac{\partial \rho_{(2)}}{\partial t} + \rho_{(0)} \frac{\partial}{\partial x_i}(u_{i(2)}) + \frac{\partial}{\partial x_i}(\rho_{(1)} u_{i(1)}) = 0$$

$$\rho_{(0)} \frac{\partial u_{i(2)}}{\partial t} + \rho_{(1)} \frac{\partial u_{i(1)}}{\partial t} + \rho_{(0)} u_{j(1)} \frac{\partial u_{i(1)}}{\partial x_j} = -\frac{\partial p_{(2)}}{\partial x_i} +$$

$$(\eta'_{(0)} + \eta_{(0)}) \frac{\partial}{\partial x_i}\left(\frac{\partial u_{k(2)}}{\partial x_k}\right) + \eta_{(0)} \frac{\partial^2 u_{i(2)}}{\partial x_j \partial x_j} + \frac{\partial}{\partial x_j}\left[\eta_{(1)}\left(\frac{\partial u_{i(1)}}{\partial x_j} + \frac{\partial u_{j(1)}}{\partial x_i}\right)\right] +$$

$$\frac{\partial}{\partial x_i}\left[\eta'_{(1)}\left(\frac{\partial u_{k(1)}}{\partial x_k}\right)\right]$$

$$\frac{\partial T_{(2)}}{\partial t} = -u_{i(1)} \frac{\partial T_{(1)}}{\partial x_i} - \frac{(\gamma-1)}{\beta_{(0)}} \frac{\partial u_{i(2)}}{\partial x_i} + \frac{\kappa_{(0)}}{\rho_{(0)} c_v} \frac{\partial}{\partial x_i}\left(\frac{\partial T_{(2)}}{\partial x_i}\right) +$$

$$\frac{1}{\rho_{(0)} c_v} \frac{\partial}{\partial x_i}\left[\kappa_{(1)} \frac{\partial T_{(1)}}{\partial x_i}\right] - q'' T_{(2)} +$$

$$\frac{\eta_{(0)}}{\rho_{(0)} c_v}\left(\frac{\partial u_{i(1)}}{\partial x_j}\right)\left(\frac{\partial u_{i(1)}}{\partial x_j} + \frac{\partial u_{j(1)}}{\partial x_i}\right) + \frac{\eta'_{(0)}}{\rho_{(0)} c_v}\left(\frac{\partial u_{k(1)}}{\partial x_k}\right)^2$$

$$p_{(2)} = \frac{c^2_{(0)}}{\gamma}(\rho_{(2)} + \beta_{(0)} \rho_{(0)} T_{(2)})$$

Equations 4. The second-order ultrasonic equations.

From the 1st order ultrasonic equations the fundamental, linear wave equations comprising dissipation due to viscosity and/or heat conduction, or when viscosity, heat conduction and radiation are neglected, the lossless linear wave equation, may be derived. The lossless linear wave equation is given as Equation 5.

$$\partial p(1) / \partial t2 = c(o)\ (\partial 2p(1) / \partial xi \partial xi) \qquad (5)$$

In Equation 5, c_o is the velocity of sound, to be understood as the velocity with which a particular phase of a small amplitude ultrasonic wave will propagate, and as c_o is a constant, all phases of the ultrasonic wave will in this linear description propagate with the same velocity c_o, the so-called equilibrium or infinitesimal velocity of sound. This is valid for small pressure amplitudes in the ultrasonic wave, which also will lead to small particle velocities u, where $u << c$. The pressure amplitude p is a function of the local density ρ and of the specific entropy s, expressed through a relation $p = p(\rho,s)$, which forms the ***Equation of State*** for the fluid. This relation may, as shown by Bjørnø [1], be expanded in a Taylor series retaining terms to 2nd order only, and as ultrasound propagation in general involves isentropic processes only, i.e. processes where $s \approx$ constant, the pressure variation around the equilibrium state pressure p_o may be expressed by Equation 6.

$$\mathbf{p - p_o = A\{(\rho - \rho_o) / \rho_o\} + (B/2)\{(\rho - \rho_o) / \rho_o\}^2}$$

where

$$\mathbf{A = \rho_o\{(\partial p/\partial \rho)_s\}_{\rho=const.} = \rho_o c_o^2 \qquad \{N/m^2\}}$$

$$\mathbf{B = \rho_o^2\{(\partial^2 p/\partial \rho^2)_s\}_{\rho=const.} \qquad \{N/m^2\}}$$

Equation 6. A Taylor series expansion of the Equation of State.

3. The second-order nonlinearity parameter B/A

Equation 6 shows the terms A and B and their dependence on the first and second derivative of p with respect ρ for constant s and derived at ρ = ρo. The ratio between B and A may, after some thermodynamic calculations be written as Equation 7,

$$\mathbf{B/A = 2\rho_o c_o\{(\partial c/\partial p)_T\}_{\rho=const.} + (2c_o T\beta c_p^{-1})\{(\partial c/\partial T)_p\}_{\rho=const.}}$$

Equation 7. The second-order non-linearity parameter.

where B/A can be seen to be governed by the derivatives of the sound velocity c with respect to p and T, for T and p being held constant, respectively. In Equation 7, β is the volume coefficient of thermal expansion, T is the absolute temperature, and c_p is the specific heat at constant pressure. The first term on the right hand side of the expression in Equation 7 is normally contributing most to B/A. ***B/A* is the second-order nonlinearity parameter**, which describes the material nonlinearity of the fluid through which a finite-amplitude ultrasonic wave propagates. As pointed out by Bjørnø [2] a close relationship exists between the nonlinearity parameter B/A and the molecular structure of the fluid involving the intermolecular or the interatomic potentials. The magnitude of B/A, which for most biological media is between 5 and 11, indicates the ability of the media to form higher harmonics to an originally sinusoidal wave of finite amplitude during its propagation away from the wave source. This ***ability to form higher harmonics***, and the ***thermodynamical expression*** Equation 7, form basis for two fundamental methods

for determination of the nonlinearity of biological materials, where B/A is used as a material characterizing parameter.

4. Distortion course of a finite-amplitude ultrasonic wave

When a period of an original sinusoidal finite-amplitude wave propagates out from an ultrasonic source and through a fluid (biological) medium, the wave will be exposed to two effects influencing its time course. These effects are (1) ***dissipation*** arising from viscosity, heat conductivity and relaxation processes and (2) ***nonlinearity*** leading to formation of higher harmonics to the fundamental frequency of the wave. These effects counteract each other and as shown on Figure 1 a distortion course of the original sinusoidal (monochromatic) wave occurs through time and space during its propagation.

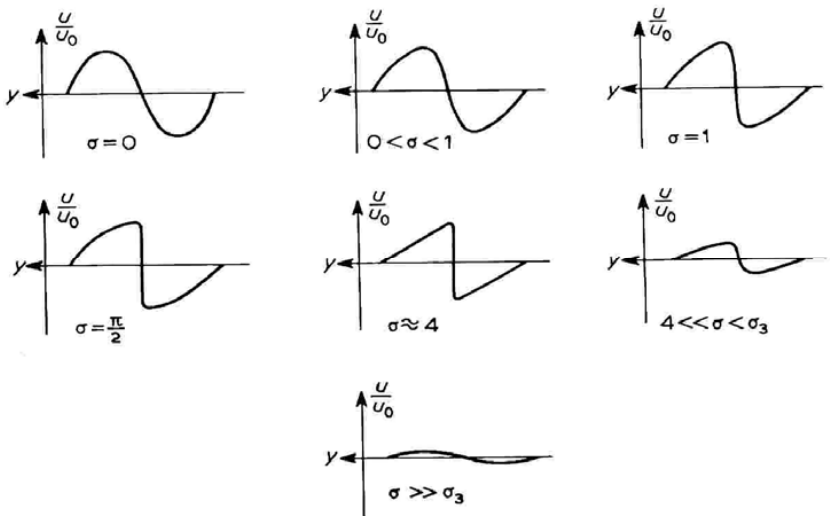

Fig.1 The nonlinear distortion course of a single period of an original finite-amplitude monochromatic wave.

The distance from the wave source is expressed by the dimensionless distance parameter σ, where the source is situated at $\sigma = 0$. The first vertical tangent to the distorted wave is formed through the 0 (zero) crossing at $\sigma = 1$. U in Figure 1 denotes the local particle velocity of the wave signal, while U_o is the particle velocity amplitude at the ultrasonic source. σ is the ratio between the source distance x and the so-called ***discontinuity distance*** ℓ, $\sigma = x/\ell$, which shows, that $x = \ell$, when the first vertical tangent to the finite-amplitude wave is formed through the zero-crossing.

$$\ell = \{(B/2A + 1)\, k\, M\}^{-1} \qquad \{m\}$$

$$c = c_o + (B/2A)\, u \qquad \{m/s\}$$

Equations 8. The discontinuity distance ℓ and the local velocity of sound c.

Equation 8 shows the relations between ℓ and B/A. A higher nonlinearity of a fluid will lead to a smaller ℓ-value and therefore a shorter distance from the ultrasonic source to the formation of the vertical tangent to the finite-amplitude wave. The expression for ℓ also shows, that ℓ is inversely proportional to the wavenumber k, and thus to the fundamental frequency of the wave, and to the acoustic Mach number M, which expresses the original amplitude of the finite-amplitude wave at the source. These characteristic features by ℓ make it an important parameter in nonlinear ultrasonics.

In Figure 1, the wave distortion takes place through various regions of space where the dissipative and nonlinear effects are influencing the distortion. Up to $\sigma = 1$, the dissipative effects are small and the nonlinear effects prevail. The accumulation of the nonlinear effects in this part of the propagation region leads to a distortion of the sinusoidal wave and to formation of increasing steepness of the wave front, eventually resulting in shock formation represented by a sawtooth wave. After $\sigma = 1$, the nonlinear and the dissipative effects cancel one another and at a source distance of $\sigma \approx 4$, stabilization of the wave shape occurs, and the sawtooth wave shape is formed. Due to the dissipation of the wave energy, the sawtooth wave profile gradually loses its wavefront steepness, and the thickness of the weak periodic shock wave increases. Finally, the wave profile returns to its original sinusoidal shape, but with a strongly reduced amplitude. This happens at much longer distance σ from the source, where the wave will propagate like an infinitesimal amplitude wave and where further amplitude reduction is governed by small-amplitude wave attenuation rules like in a sound wave.

The distortion course of the wave shown in Figure 1, where local phases of the wave will possess a local particle velocity increasing with the local ultrasonic pressure, will lead to a sort of "overtaking effect", where parts (phases) of the wave are moving along (convected) with a higher local velocity of sound c than the phase velocity c_o of the zero-crossing parts of the wave. The sound velocity increment can in Equation 8 be seen to depend on the product of the local particle velocity u and the nonlinearity parameter B/A. Therefore, the distortion of the original sinusoidal wave during its propagation receives contributions from two effects, the ***convective*** and the ***material nonlinearity*** effects. For $B/A > 2$, which is the case for most liquids and biological materials, the distortion contribution from the material nonlinearity, represented by B/A from the nonlinear equation of state, Equation 6, will be stronger than the convective contribution.

Whether the shape of the finite-amplitude sinusoidal wave will change through all regions shown in Figure 1 will depend on the material (or structural) nonlinearity of the fluid expressed by B/A, on the initial pressure amplitude p_o of the ultrasonic wave, on its fundamental frequency f_o, and on the strength of the dissipative qualities of the fluid expressed by its dissipation constant b given in Equations 9.

$$b = (4/3)\eta + \eta' + \kappa(1/c_v + 1/c_p) \quad \{Ns/m^2\}$$

$$\Gamma = (B/A + 2)\, p_o/2\pi f\, b = (B/A + 2)\, Re_a$$

Equations 9. The dissipation constant b and the Gol'dberg Number Γ.

The expression for b in Equations 9 shows, that the dissipation originates from viscosity and heat conductivity – the classical dissipation factors – while relaxation effects, in particular molecular relaxation, demands an extra term, unless the relaxation effects form a part of the bulk viscosity term η'. As shown by Gol'dberg [3], a criterion for that shock formation, i.e. the sawtooth wave shape in Figure 1, will take place is, that the so-called Gol'dberg number Γ in Equations 9 will have such a magnitude that $\Gamma > 1$. Γ represents the two main distortion effects influencing the finite-amplitude ultrasonic wave, namely the nonlinear effects represented by B/A, and the dissipative effects represented by b. In order to connect the Gol'dberg number Γ with the general convective and dissipation effects in Fluid Mechanics represented by the ***acoustic Reynolds number*** Re_a, Equations 9, also shows Γ expressed by Re_a. Therefore, when a sinusoidal wave of not too high initial amplitude propagates through a thermoviscous fluid, the dissipation effects will lead to the fact that the sawtooth wave formation will be avoided. For higher initial wave amplitudes the sawtooth shape will occur, and when sufficiently high initial wave amplitudes exist, the later amplitudes of the distorted, original sinusoidal, ultrasonic wave will become relatively independent of the initial amplitude, and a so-called ***acoustical saturation*** has been achieved. When this occurs, a further increase in the

pressure amplitude p_o at the ultrasonic source will lead to the same amplitude of the distorted wave, particularly due to near-field absorption, regardless of how much p_o is increased.

The wave distortion shown in the time domain in Figure 1, will in the frequency domain be represented by formation of higher harmonics to the fundamental sinusoidal frequency f_o. The formation of the 2nd and 3rd harmonics to the fundamental frequency of a sinusoidal wave is given in Figure 2.

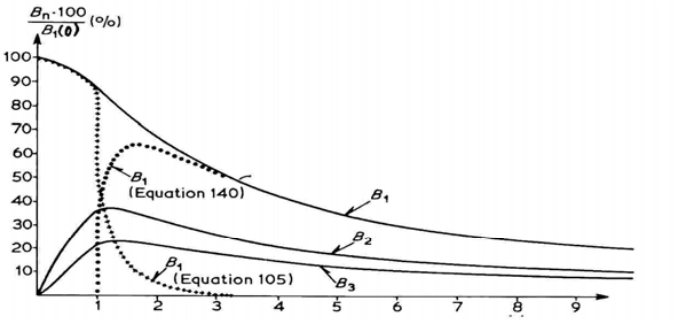

$$\sigma = x/\ell = (B/2A + 1)\, u_o\, k\, x / c_o$$

$$\alpha = 2\pi^2 f^2 b (\rho_o c_o^3)^{-1} \qquad \{m^{-1}\}$$

Fig.2 The dimensionless Fourier coefficient as a function of σ.

Figure 2 shows the dimensionless amplitude (Fourier coefficient) variation as a function of the dimensionless source distance parameter σ for the fundamental frequency wave B_1 and for its second and third harmonics B_2 and B_3, respectively. The equations 105 and 140 referred to in Figure 2 are the Fubini and Fay solutions, respectively, to the nonlinear wave equations on Equations 4, as discussed by Bjørnø [1]. As can be seen from Figure 2, that while the amplitude B_1 of the fundamental frequency wave reduces continuously for increasing source distance, due to the dissipation influence and the transfer of energy to its harmonics, the harmonic's amplitudes first increases to just after $\sigma = 1$, while B_1 and B_2 then decreases due to dissipation. As the ***infinitesimal amplitude absorption coefficient*** α given in Figure 2 depends on the frequency f, squared, the attenuation of the harmonics will be governed by 4α and 9α, respectively, for the 2nd and 3rd harmonics. This leads to a faster dissipative reduction in the harmonics amplitudes than in the fundamental frequency wave. Therefore, the nonlinear transfer of energy from the fundamental frequency to its harmonics will increase the effect of attenuation on the fundamental frequency wave.

While the ***thermodynamical method*** exploits the expression for ***B/A***, Equation 7, with individual determination of the factors in the two terms, and where the derivatives of the velocity of sound c with respect to pressure p and temperature T for constant T and p, respectively, are the key parameters, then the ***finite-amplitude method*** is based on measurements of the 2nd harmonic's pressure amplitude $p_2(x)$ as a function of the source distance x. By extrapolation back to the source at $x = 0$, the ratio $p_2(x)/xp_o$, where p_o is the ultrasonic wave pressure amplitude at the source, can be formed as given in Equation 10.

$$\left[\frac{p_2(x)}{xp_s^2}\right]_{xp_s^2 \to o} = \frac{(2 + B/A)\pi f}{2\rho_o c_o^3} \exp[-(\alpha_1 + \alpha_2/2)x]$$

Equation 10. Formation of second harmonic pressure amplitude p_2 as a function of source distance x.

In Equation 10, α_1 and α_2 denote the attenuation coefficient for the fundamental frequency ultrasonic wave and its first harmonic, respectively. The use of the expression for *B/A* in Equation 10 demands that the attenuation of the fundamental frequency wave and its 2nd harmonic amplitudes are mutually independent and that the rate of change with propagation distance of the 2nd harmonic amplitude is the sum of changes caused by the nonlinear generation of the 2nd harmonic and its subsequent attenuation.

Experimental determination of *B/A* by use of the finite-amplitude method will normally involve the use of two ultrasonic piston transducers positioned coaxially and with a few centimetres of distance between the transducer surfaces. This distance is occupied partly or fully by the biological medium to be investigated. Due to the short source-receiver separation distance, the influence of diffraction effects as well as phase cancellation across the receiver surface can be expected, and corrections have to be introduced accordingly. Values of *B/A* for biological materials measured and published by various authors are collected in Table 1, where *F.A.* refers to the use of the finite-amplitude procedure, while *Therm.* refers to the use of the thermodynamical method, see Bjørnø [2].

Attempts have also been made by Ichida et al [4] to develop a ***real-time nonlinear parameter tomographic method*** based on the interaction between two waves of different frequencies, a pump wave of finite amplitude and a probing wave of low amplitude, and a subsequent real-time phase demodulation of the detected probing wave. A discussion of the method and its applicability can be found in Bjørnø and Lewin [5].

Table 1. *B/A*-values for some biological media, see Bjørnø [2].

Some *B/A* values for biological materials

Biological material (and state)	Method[a]	*B/A* (and uncertainty)
Bovine serum albumin (BSA) (20 g/100 cm^3, 25°C)	Therm.	6.23 (± 0.25)
BSA (22 g/100 cm^3, 30°C)	F.A.	6.45 (± 0.30)
BSA (38.9 g/100 cm^3, 30°C)	F.A.	6.64
BSA (38.9 g/100 cm^3, 30°C)	Therm.	6.68 (± 0.2)
Haemoglobin (50%, 30°C)	F.A.	7.6
Whole porcine blood (12% haemoglobin, 7% plasma proteins, 30°C)	F.A.	6.2 (± 0.25)
Beef liver (Whole, 23°C)	F.A.	7.75 (± 0.4)
Beef liver (Homogenized, 23°C)	F.A.	6.8 (± 0.4)
Beef liver (Whole, 30°C)	F.A.	6.42
Beef liver (Whole, 30°C)	Therm.	6.88
Beef liver (Whole, 30°C)	Therm.	6.54 (± 0.2)
Dog liver (30°C)	F.A.	7.6 – 7.9 (± 0.8)
Pig liver (25°C)	F.A.	6.7 (± 1.5)
Human liver (Normal, 30°C)	F.A.	7.6 (± 0.8)
Human liver (Congested, 30°C)	F.A.	7.2 (± 0.7)
Pig fat	Therm.	10.9
Pig fat	F.A.	11.0–11.3
Human breast fat (22°C)	Therm.	9.21
Human breast fat (30°C)	Therm.	9.91
Human breast fat (37°C)	Therm.	9.63
Canine spleen	F.A.	6.8
Dog spleen	F.A.	6.8 (± 0.7)
Human spleen (Congested)	F.A.	7.8
Human spleen (Normal, 30°C)	F.A.	7.8 (± 0.8)
Beef brain (30°C)	F.A.	7.6
Beef heart (30°C)	F.A.	6.8–7.4
Pig muscle (30°C)	F.A.	7.5–8.1
Pig muscle (25°C)	F.A.	6.5 (± 1.5)
Dog kidney (Normal, 30°C)	F.A.	7.2 (± 0.7)
Canine kidney (30°C)	F.A.	7.2
Human multiple myeloma (22°C)	F.A.	5.6
Human multiple myeloma (30°C)	F.A.	5.8
Human multiple myeloma (37°C)	F.A.	6.2

Prior to shock formation, the unfocused harmonic components to an original sinusoidal finite-amplitude ultrasonic wave have far-field ***beam patterns*** (directivity functions) $D_n(\theta)$, where n is the harmonic number and θ denotes the angle to the acoustic axis of the ultrasonic source, as given in Equations 11, see Bjørnø [1].

$$D_n(\theta) = \{D_{n-1}(\theta)\}^n$$
$$B_n = 2\{n(1 + \sigma)\}^{-1}$$

Equations 11. The directivity function $D_n(\theta)$ and the harmonic amplitude B_n.

From Equations 11 it can be seen, that the beam patterns of the 2nd harmonic is the square of the beam patterns of the fundamental sinusoidal finite-amplitude ultrasonic wave, and that each successive harmonic has an increasing directivity and therefore, narrower beams with increasing sidelobe suppression. The beam patterns of the higher harmonics can be used for improvements of the resolution in ultrasonic image formation.

After $\sigma = 1$, each harmonic begins to show finite-amplitude attenuation in its main lobe, which leads to some beam broadening and a decrease in the sidelobe suppression compared with the beam structure in the dimensionless source distance region $0 < \sigma < 1$. When the sawtooth wave formation has been achieved, the amplitude of the harmonics B_n will be inversely proportional to the harmonic's number as shown in the expression for B_n in Equations 11, see Bjørnø [1].

5. Focused ultrasonic fields

Focused ultrasonic fields have found wide-spread application over recent years for instance in lithotripters for removal of body stones, in ultrasonic surgery and in ultrasonic microscopes. The propagation of finite-amplitude bounded ultrasonic waves in a dissipative medium and including nonlinear and diffraction effects can be described by use of the so-called K-Z-K equation, see Kuznetsov [6], and the solution to this equation for focused ultrasonic fields in some biological media has been found by Neighbors and Bjørnø [7]. The K-Z-K equation is given as Equation 12, where the 2nd term on the left hand side includes the diffraction effects in the ultrasonic field, while the 3rd term includes the thermoviscous absorption effects. The nonlinear effects are included in the term on the right hand side of the equation. The derivation of the K-Z-K equation, Equation 12, assumes a well-collimated ultrasonic beam, i.e. $ka >> 1$, where k is the wave number.

$$4(\partial 2p/\partial\tau\partial\sigma) - \Delta 2p - 4\alpha ro(\partial 3p/\partial\tau 3) = 2(ro/\ell)(\partial 2p2/\partial\tau 2) \qquad (12)$$

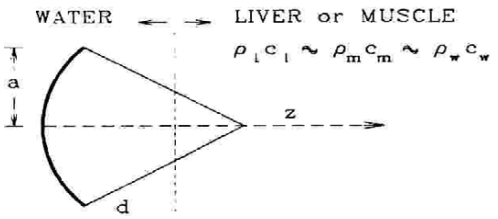

Fig.3 Focused finite-amplitude ultrasonic field penetrating from water into liver/muscle tissue [7].

The geometry used in applying the K-Z-K equation to ***focused ultrasonic fields of finite-amplitude*** is shown in Figure 3. Here a is the aperture radius of the focused source, while z describes the distance from the source. d is the radius of curvature for the focused source. In Figure 3, the ultrasonic field originates at a concave source and travels in the positive z direction. Maximum nonlinear interaction occurs around the focal zone at $z = d$, and the source is

assumed to be axisymmetric with a linear focusing gain $G = r_o/d$, where r_o is the Rayleigh distance, which is a characteristic distance in the ultrasonic field of a piston source, $r_o = a^2/\lambda$, where λ is the ultrasonic wavelength.

After appropriate boundary conditions have been defined at the concave source and after a coordinate transformation to enhance the computational efficiency has been introduced by Neighbors and Bjørnø [7], the K-Z-K equation, Equation 12, may be reformulated to the form given as Equation 13, which accounts for nonlinearity, diffraction and absorption to an equal order of magnitude.

$$\partial 2p/\partial\tau\partial\sigma - \Delta 2p/4G - K1(\partial 3p/\partial\tau 3) = (K2/2)(\partial 2p/\partial\tau 2) \qquad (13)$$

A numerical solution to the K-Z-K equation, Equation 13, for a focal gain G = 72.5, and where A = K1 = 1.11 and B = K2 = 1.06, is given on Figure 4. These values for G, A and B were selected for comparison with a study of acoustic microscopy by Ruger [8], and the directivity of the focused ultrasonic beam has been calculated by Bjørnø and Neighbors [9] at the focal point, z = d, and the fundamental monochromatic ultrasonic wave and its harmonics are shown on Figure 4.. This figure also shows the improved directivity and the reduced sidelobes of the harmonics to a 3 MHz fundamental wave.

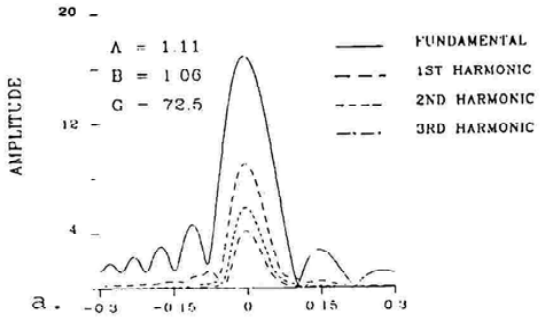

Fig.4 A numerical solution to the K-Z-K Equation for a focused ultrasonic field [9].

The axial pressure amplitude distribution for a 500 kHz monochromatic, finite-amplitude wave propagating through water and liver or muscle tissue, as shown on Figure 3, when the focal gain G = 100, and the on-axis pressure variation p is normalized by division with 100po, where po is the peak pressure at the concave source, is calculated by Neighbors and Bjørnø [7] and is shown in Figure 5. Here σ' = 0 is the focal point, and the negative values of σ' indicates locations before the focal point.

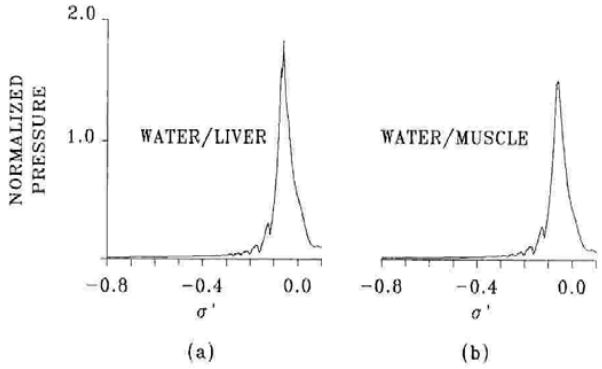

Fig.5 Normalized pressure variation around the focal point for various water-tissue combinations from Figure 3 [7]

Figure 5 shows the strong increase in the focused pressure amplitude p near the focal point, and that the maximum pressure amplitude is achieved just before the focal point due to the increased absorption on higher harmonics formed when the focal region is approached.

6. The parametric acoustic array

A superior beam quality may also be obtained when two finite-amplitude waves of different frequencies are superimposed and interact nonlinearly with each other. This is for instance the case in a ***parametric acoustic array*** suggested by Westervelt [10], where for instance two high-frequency, plane, collimated primary waves interact in a fluid, producing sum and difference frequency beams without sidelobes. In particular the narrow difference-frequency beam has been of interest and has found applications among other things in underwater sonar technology, as discussed by Bjørnø [11]. Based on the solutions to Lighthill's [12] inhomogeneous wave equation for aerodynamic generation of sound, Westervelt [10] found the difference-frequency pressure amplitude p_s as a function of distance R from an observation point to the projector emitting the primary waves and as a function of the angular coordinate θ of the observation point. This difference-frequency pressure amplitude p_s is given in Equation 14.

$$ps(R,\theta) = \pi fs2po2S(2poco4R)\text{-}1\{1 + B/2A\}\ \{\alpha 2 + ks2sin4(\theta/2)\}\text{-}½ \qquad (14)$$

In the far-field, the half-power beamwidth of the parametric acoustic array, $\theta_h \approx 2(\alpha/k_s)^{½}$, will depend on the absorption coefficient α and the difference-frequency wave number k_s, only. This dependence shows that a narrowing of the difference-frequency beam will take place for a decrease in the primary frequencies, due to the decrease in α, opposite to what is the case for a conventional, linear transducer beam. Further, a decrease of the difference-frequency beamwidth will follow an increase in the difference frequency. The interaction region between the two high-frequency, plane, collimated primary waves is shown in Figure 6, where the virtual sources for formation of the difference-frequency wave are distributed along the interaction region. This distribution of virtual signal sources has been likened to an end-fire array, where a high amplitude (directivity) is produced in the x-direction.

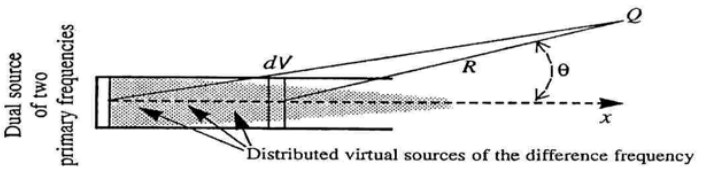

Fig.6 The interaction region between two high-frequency primary waves to form the difference-frequency wave.

Due to the fact that the effective array length can be made very large, highly directive difference-frequency beams can be produced by a projector not large compared to the difference-frequency wavelength. The exponential shading resulting from the primary wave absorption will also lead to very low sidelobe pressure levels. Moreover, considerable frequency agility characterizes the parametric acoustic array.

As it, however, is difficult to produce collimated finite-amplitude primary waves, and as measurements most frequently take place in the interaction region between the primary waves or in their near-field, where diffraction effects dominates over viscous effects, another expression, which permits calculations of the difference-frequency pressure amplitude p_s in the interaction region, was developed by Muir and Villette [13] and is given in Equation 15.

$$ps(x,t) = \text{-}(1 + b/2A)\{4\pi poco4\}\text{-}1\lfloor dV/R(\partial 2/\partial t2\{pi2(x,t - R/co)\}) \qquad (15)$$

In Equation 15, R is the distance between the field point Q in Figure 6, and dV is the volume element of the interaction region between the primary waves of pressure amplitudes p_i. The 3D scattering integral in Equation 15 takes full account of the diffraction effects, see Bjørnø [11]. While the beam qualities of the parametric array are attractive, the ***parametric conversion efficiency*** for the energy transfer from the primary waves to the difference-frequency wave puts some limitations on the applicability of the array, as nearly 40 dB in amplitude level difference exists between the primary waves and their difference-frequency wave. This power loss can only be defended when the extremely high directivity of the difference-frequency wave at low frequencies for smaller transducer sizes and the lack of sidelobes are of primary importance. In spite of its low conversion efficiency, attempts have been made by Bjørnø and Grinderslev [14] to exploit the parametric array in medical echoscanning, in particular with the aim to find small metal pieces in the body of wounded soldiers.

The companion papers by P.A.Lewin and A. Nowicki (somewhere in this volume) are focused on the application of nonlinear acoustics in ultrasound metrology and selected applications of nonlinear wave propagation in ultrasound imaging.

References

[1] Bjørnø, L., *Nonlinear Acoustics*, in R.W.B. Stephens an H.G. Leventhall (Eds.), Acoustics and Vibration Progress, Vol. 2, Chapman and Hall, London, pp 101 – 198, 1976.
[2] Bjørnø, L., *Characterization of biological media by means of their non-linearity.* Ultrasonics, Vol. 24, pp 254 - 259, 1986.
[3] Gol'dberg, Z.A., *On the propagation of plane waves of finite amplitude.* Sov. Phys. (Acoustics), Vol. 2, pp 346 -352, 1956.
[4] Ichida, N., Sato, T., Miwa, H. And Kurakami, K., *Real-time nonlinear parameter tomography using impulsive pumping waves.* IEEE Trans. Sonics Ultrasonics, Vol. SU-31, (6), pp. 635 – 642, 1984.
[5] Bjørnø, L. and Lewin. P. A., *Measurement of nonlinear acoustic parameters in tissue.* In J.F. Greenleaf (Ed.), Tissue Characterization with Ultrasound, Vol. I, CRC Press, pp 141 – 163, 1986.
[6] Kuznetsov, V.P., *Equations of nonlinear acoustics.* Sov. Phys. (Acoustics), Vol. 16, pp. 467 – 470, 1971
[7] Neighbors, T.H. and Bjørnø, L., *Monochromatic focused sound fields in biological media.* J. Lithotripsy and Stone Disease, Vol. 2, (1), pp 4 – 16, 1990.
[8] Ruger, D., *Resolution beyond the diffraction in the acoustic microscope.* J. Appl. Phys., Vol. 56, pp. 1338 – 1146, 1984.
[9] Bjørnø, L. and Neighbors, T.H., *A parameter study of focused sound fields in active media.* Proc. EUROMECH 241 on Nonlinear Waves in Active Media, Tallinn, pp 3 – 10, 1988.
[10] Westervelt, P.J., *Parametric acoustic array.* J. Acoust. Soc. Amer., Vol. 35, pp 535 – 537, 1963
[11] Bjørnø, L., *40 years of Nonlinear Underwater Acoustics.* ACTA Acustica united with Acustica, Vol. 88, pp 771 – 775, 2002.
[12] Lighthill, M.J., *On sound generated aero-dynamically. I: General Theory.* Proc. Roy. Soc. (London), Vol. 211A, pp 564 – 587, 1952.
[13] Muir, T.G. and Willette, J.G., *Parametric acoustic transmitting arrays.* J. Acoust. Soc. Amer., Vol. 52, pp 1481 – 1486, 1972.
[14] Bjørnø, L. and Grinderslev, S., *Parametric echoscanner for medical diagnosis.* Journal de Physique, Colloque C8, Supplémentau n° 11, Tome 40, pp 111 - 118, 1979